APPENDIX A: TABLES AND SPECTROSCOPY

REFERENCES

Baroch D., et al., 2021, A&A, 653, A49
Beers T. C., Preston G. W., Shectman S. A., Doinidis S. P., Griffin K. E., 1992, AJ, 103, 267
Bergeron P., Kilic M., Blouin S., Bédard A., Leggett S. K., Brown W. R., 2022, ApJ, 934, 36
Blouin S., Dufour P., 2019, MNRAS, 490, 4166
Bonavita M., et al., 2020, MNRAS, 494, 3481
Bowler B. P., et al., 2021, AJ, 161, 106
Caron A., Bergeron P., Blouin S., Leggett S. K., 2023, MNRAS, 519, 4529
Crepp J. R., Johnson J. A., Howard A. W., Marcy G. W., Gianninas A., Kilic M., Wright J. T., 2013, ApJ, 774, 1
Crepp J. R., et al., 2018, ApJ, 864, 42
Delfosse X., Forveille T., Beuzit J. L., Udry S., Mayor M., Perrier C., 1999, A&A, 344, 897
Dreizler S., Werner K., 1996, A&A, 314, 217
Elms A. K., Tremblay P.-E., Gänsicke B. T., Koester D., Hollands M. A., Gentile Fusillo N. P., Cunningham T., Apps K., 2022, MNRAS, 517, 4557
Fajardo-Acosta S. B., et al., 2016, ApJ, 832, 62
Farihi J., Bond H. E., Dufour P., Haghighipour N., Schaefer G. H., Holberg J. B., Barstow M. A., Burleigh M. R., 2013, MNRAS, 430, 652
Gentile Fusillo N. P., et al., 2021, MNRAS, 508, 3877
Giammichele N., Bergeron P., Dufour P., 2012, ApJS, 199, 29
Gianninas A., Bergeron P., Ruiz M. T., 2011, ApJ, 743, 138
Gies D. R., et al., 2020, ApJ, 902, 25
Gizis J. E., 1998, AJ, 115, 2053
Hirsch L. A., et al., 2019, ApJ, 878, 50
Holberg J. B., Oswalt T. D., Sion E. M., Barstow M. A., Burleigh M. R., 2013, MNRAS, 435, 2077
Jao W.-C., Henry T. J., Subasavage J. P., Winters J. G., Gies D. R., Riedel A. R., Ianna P. A., 2014, AJ, 147, 21
Kilic M., et al., 2010, ApJS, 190, 77
Koester D., 2010, Mem. Soc. Astron. Italiana, 81, 921
Limoges M. M., Lépine S., Bergeron P., 2013, AJ, 145, 136
Limoges M. M., Bergeron P., Lépine S., 2015, ApJS, 219, 19
Monteiro H., Jao W.-C., Henry T., Subasavage J., Beaulieu T., 2006, ApJ, 638, 446
O'Brien M. W., et al., 2023, MNRAS, 518, 3055
Putney A., 1997, ApJS, 112, 527
Tremblay P. E., et al., 2020, MNRAS, 497, 130
Winters J. G., et al., 2020, AJ, 159, 290
Zuckerman B., Becklin E. E., Macintosh B. A., Bida T., 1997, AJ, 113, 764
van Leeuwen F., 2007, A&A, 474, 653
van den Besselaar E. J. M., et al., 2007, A&A, 466, 1031

This paper has been typeset from a TEX/LATEX file prepared by the author.

Table A1. The catalogue of 1073 *Gaia* white dwarfs within 40 pc, which is accessible online at this link. See Table 1 for details.

Table A2. White dwarf candidates within 40 pc in the Gentile Fusillo et al. (2021) DR3 catalogue that do not have spectroscopic follow-up.

WD J Name	DR3 Source ID	Parallax	P_{WD}	*Gaia* T_{eff}	*Gaia* $\log(g)$
041359.12−212222.67	5090109228757394048	27.87 (0.08)	0.66	4000 (50)	7.11 (0.05)
081219.58−261639.46	5694534861029977472	26.5 (0.8)	0.30	5050 (20)	6.88 (0.09)
095953.92−502717.75	5405389966089801984	26.57 (0.04)	1.00	6950 (140)	8.12 (0.05)
115007.08+240403.54	4004185576130620288	33.2 (0.3)	1.00	3600 (200)	8.5 (0.1)
∗224600.88−060947.02	2611515835965491968	27 (1)	0.79	–	–

∗: This system is likely to be a brown dwarf.

Table A3. Confirmed white dwarfs and candidates in the Gentile Fusillo et al. (2021) DR3 catalogue that are within $1\sigma_{\varpi}$ of 40 pc.

WD J Name	DR3 Source ID	Parallax	P_{WD}	SpT	Reference
014240.09−171410.85	5142336825646176256	24.97 (0.09)	1.00	DAH	O'Brien et al. (2023)
054858.25−750745.20	4648527839871194880	24.97 (0.09)	–	DZH	O'Brien et al. (2023)
055231.03+164250.27	3349849778193723008	24.97 (0.04)	1.00	DBA	Tremblay et al. (2020)
080247.02+564640.62	1081514379072280320	24.9 (0.2)	0.99	DC	Tremblay et al. (2020)
100819.19+121813.94	3881550619014086912	23 (3)	1.00	–	–
∗102834.88−000029.39	3831059120921201280	24.997 (0.026)	0.03	DA+M	Gianninas et al. (2011)
122257.77−742707.70	5838312052354944256	24.97 (0.07)	0.99	DA	O'Brien et al. (2023)
133340.50−370550.65	6162813873991704960	24.99 (0.07)	0.99	–	–
134118.69+022737.01	3713218786120541824	24.96 (0.09)	0.99	DQ	Kilic et al. (2010)
180218.60+135405.46	4496751667093478016	25.00 (0.04)	0.99	DAZ	Tremblay et al. (2020)
183010.48−244209.53	4077104740685645056	24 (1)	1.00	–	–
193500.68−172443.11	4180014832789446400	25.0 (0.2)	1.00	DC	Tremblay et al. (2020)
193501.33−072527.42	4207055367062840320	24.9 (0.2)	0.96	DC	This work
214810.74−562613.14	6460523071166427392	24.98 (0.08)	1.00	DAH	O'Brien et al. (2023)
222919.46−444138.86	6520516480027596288	24.97 (0.03)	1.00	DA	Beers et al. (1992)

∗: This system has a low P_{WD} due to the M-dwarf companion.

Table A4. White dwarfs within 40 pc that are not in the Gentile Fusillo et al. (2021) DR3 catalogue.

DR3 Source ID	WD Name	Parallax	SpT	SpT Reference	Note
–	Procyon B	285 (1)	DQZ+F	Limoges et al. (2015)	(1)
1355264565043431040	WD 1708+437	131.6 (0.4)	WD+M	Delfosse et al. (1999)	(2)
4937000898856154624	WD 0210−510	92.6 (0.1)	DQ	Farihi et al. (2013)	(3)
975968340910692608	WD 0727+482B	88.72 (0.03)	DA	Limoges et al. (2015)	(4)
975968340912517248	WD 0727+482A	88.72 (0.03)	DA	Limoges et al. (2015)	(4)
3223516063958808064	GJ 207.1	63.36 (0.05)	WD+M	Baroch et al. (2021)	(2)
1005873614080407296	LHS 1817	61.43 (0.05)	WD+M	Winters et al. (2020)	(2)
2185710338703934976	WD 2003+542	60.30 (0.03)	WD+M	Gizis (1998)	(2)
4788741548375134336	WD 0419−487	47.2 (0.02)	DA+M	Gianninas et al. (2011)	(2)
1362295082910131200	HD 159062B	46.19 (0.01)	WD+G	Hirsch et al. (2019)	(4)
2274076301516712704	WD 2126+734B	44.91 (0.07)	DC	Zuckerman et al. (1997)	(3)
6431977687725247104	SCR J1848−6855	43.9 (0.1)	WD+M	Jao et al. (2014)	(2)
3701290326205270528	WD 1214+032	42.77 (0.04)	DA	Limoges et al. (2015)	(3)
2983256662868370048	GJ 3346 B	42.24 (0.04)	WD+K	Bonavita et al. (2020)	(3)
–	Regulus B	41.1 (0.4)	WD+B	Gies et al. (2020)	(1)
3729017810434416128	HD 114174 B	37.87 (0.02)	WD+G	Crepp et al. (2013)	(2)
1548104507825815296	WD 1213+528	34.95 (0.02)	DA+M	Limoges et al. (2015)	(2)
1550299304833675392	WD 1324+458	32.77 (0.02)	DA+M	van den Besselaar et al. (2007)	(2)
5389590533737966208	WD 1108−408	32.5 (0.2)	DC	Monteiro et al. (2006)	(3)
6665685378201412992	CD−53 8345B	31.3 (0.08)	DA	O'Brien et al. (2023)	(3)
4478524169500496000	HD 169889	28.27 (0.03)	WD+G	Crepp et al. (2018)	(2)
–	WD 1634−573	27.9 (0.2)	DOA+K	Dreizler & Werner (1996)	(1)
1962707287281651712	PM J22105+4532	27.76 (0.09)	DC	Limoges et al. (2013)	(3)
2643862402903084544	12 Psc B	27.53 (0.02)	WD+G	Bowler et al. (2021)	(2)
3845263368043086080	WD 0911+023	27.1 (0.6)	WD+B	Holberg et al. (2013)	(2)
3817534337626005632	WD 1120+073	27.0 (0.5)	DC	Limoges et al. (2015)	(4)
759601941671398272	WD 1133+358	25.91 (0.06)	DC+M	Putney (1997)	(2)
3000597125173673088	PM J06157−1247	25.8 (0.1)	WD+M	Fajardo-Acosta et al. (2016)	(2)

Notes: (1) Missing entirely from *Gaia* DR3, (2) Unresolved white dwarf plus main sequence binary, (3) Missing or incorrect colours, (4) Missing five-parameter astrometry. For many binaries, parallaxes are of the companion. Where no *Gaia* ID is available, parallaxes are from *Hipparcos* (van Leeuwen 2007). A white dwarf that has not been spectroscopically confirmed is denoted as WD.

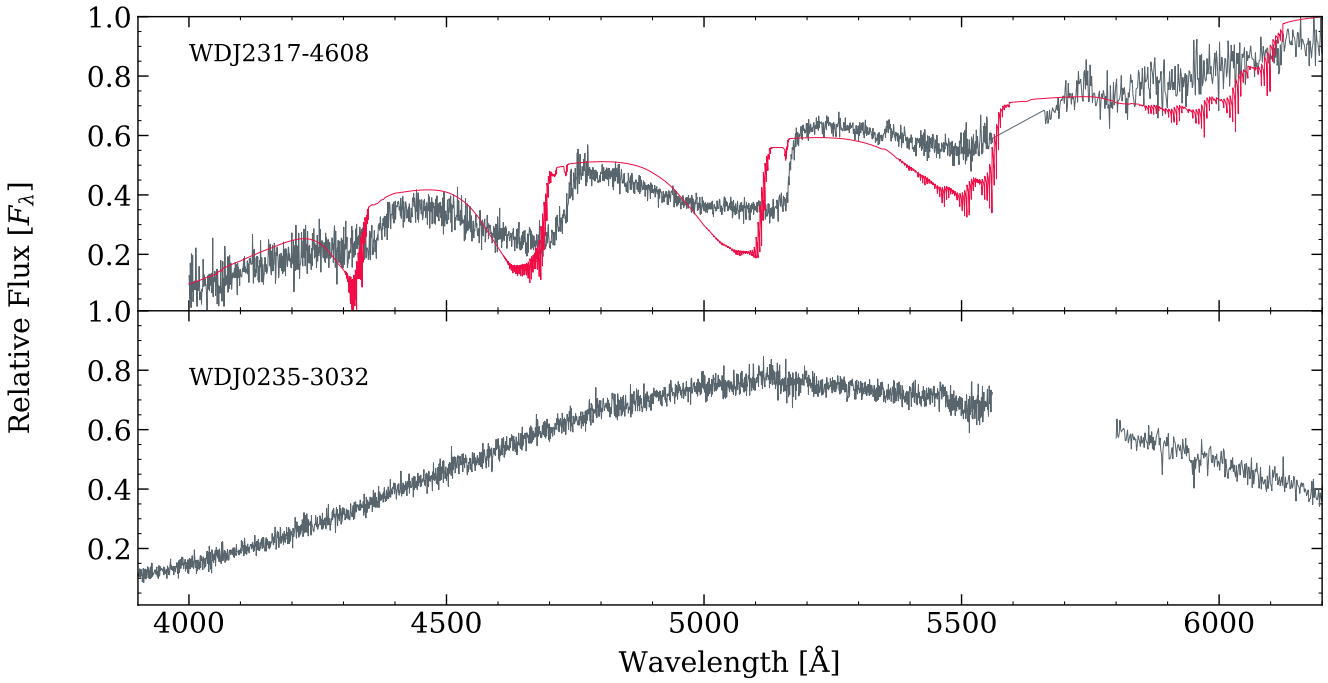

Figure A1. Spectra of two white dwarfs observed with X-Shooter. Top: the DQpec white dwarf **WD J2317−4608**, with our best-fit model spectrum over-plotted in red, based on DQ models (Koester 2010). Bottom: the IR-faint DC white dwarf **WD J0235−3032**.

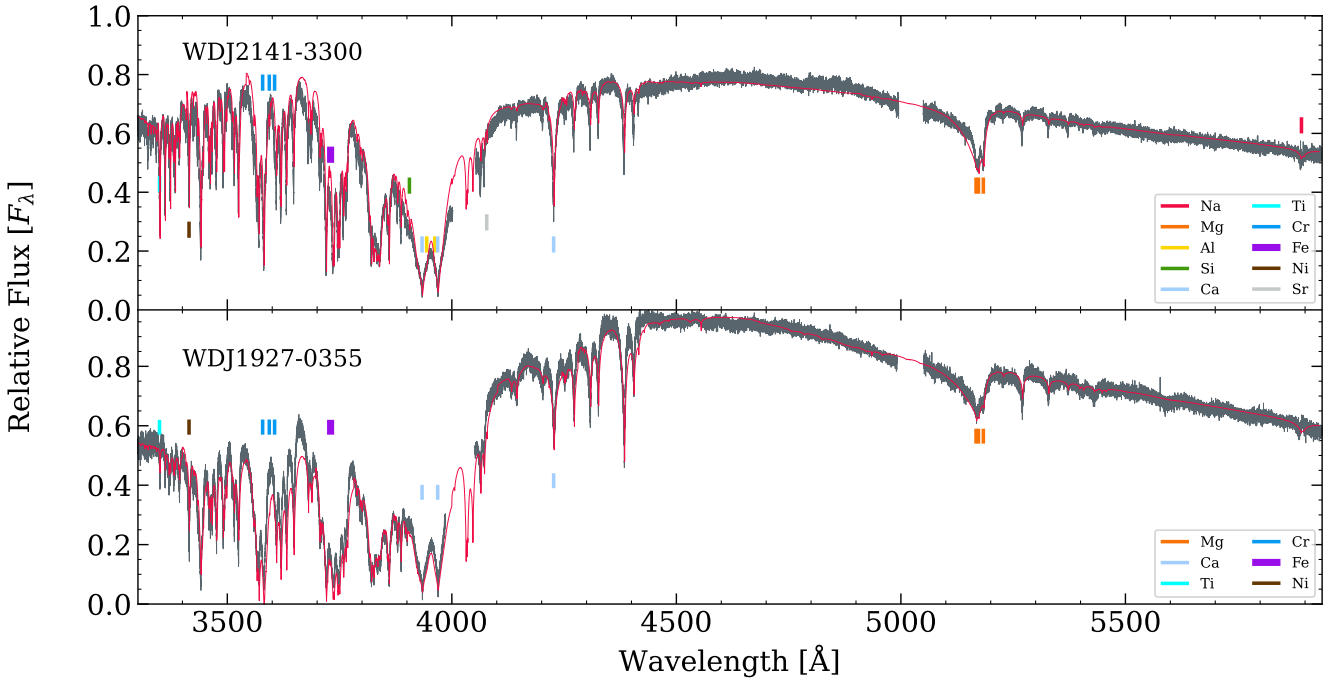

Figure A2. Spectra of two metal-polluted white dwarfs, **WD J2141−3300** and **WD J1927−0355**, observed with HIRES. A few prominent metal features are highlighted with ticks. Our best-fit model spectra are over-plotted in red (Koester 2010).

Table A5. White dwarfs within 40 pc with unreliable *Gaia* parameters. Best-fit parameters are instead taken from literature.

WD J Name	Parallax [mas]	SpT	$T_{\rm eff}$ [K]	Mass [$M_\odot$]	Description	Reference
021348.83−334530.03	53.33 (0.06)	DAZ	5150 (150)	0.4 (0.1)	(1)	This work
023538.55−303225.52	30.6 (0.2)	DC	–	–	(2)	This work
022432.27−285459.46	34.5 (0.1)	DC	4880 (160)	1.071 (0.003)	(2)	Bergeron et al. (2022)
034646.52+245602.67	25.3 (0.2)	DC	3640 (60)	0.423 (0.007)	(2)	Bergeron et al. (2022)
050600.41+590326.89	27.7 (0.3)	DC	–	–	(2)	This work
063038.60−020550.49	46.72 (0.03)	DA+M	6910 (140)	0.53 (0.1)	(1)	Gianninas et al. (2011)
064509.30−164300.72	374.5 (0.2)	DA	25 970 (380)	0.98 (0.03)	(1)	Giammichele et al. (2012)
075508.95−144550.95	25.55 (0.02)	DA+M	19440 (290)	0.58 (0.02)	(1)	Gianninas et al. (2011)
085357.69−244656.23	38.8 (0.1)	DC	3740 (40)	0.672 (0.003)	(2)	Bergeron et al. (2022)
090208.37+201051.57	26.1 (0.1)	DQ	5500 (110)	0.71 (0.01)	(3)	Blouin & Dufour (2019)
101141.58+284559.07	67.88 (0.06)	DQpecH	4340 (170)	0.70 (0.06)	(3)	Blouin & Dufour (2019)
104410.24−691818.08	34.18 (0.02)	DA+M	22570 (330)	0.54 (0.02)	(1)	Gianninas et al. (2011)
110217.52+411321.18	28.7 (0.3)	DC	3790 (20)	0.56 (0.01)	(2)	Caron et al. (2023)
122048.70+091413.08	26.7 (0.3)	DC	3890 (60)	1.081 (0.008)	(2)	Bergeron et al. (2022)
130503.44+702243.05	28.9 (0.2)	DC	–	–	(2)	Tremblay et al. (2020)
140324.75+453333.02	29.1 (0.2)	DC	4820 (20)	1.184 (0.003)	(2)	Bergeron et al. (2022)
155647.51−080601.24	30.6 (0.2)	DC	4880 (110)	1.054 (0.004)	(2)	Bergeron et al. (2022)
165401.26+625354.91	32.5 (0.1)	DC	4990 (30)	1.049 (0.002)	(2)	Bergeron et al. (2022)
192206.20+023313.29	25.4 (0.3)	DZ	3340 (50)	0.57 (0.03)	(2)	Elms et al. (2022)
195211.78−732235.48	31.2 (0.3)	DC	–	–	(2)	O'Brien et al. (2023)
201231.78−595651.67	60.80 (0.03)	DC	4910 (210)	0.44 (0.01)	(2)	Giammichele et al. (2012)
214756.59−403527.79	35.8 (0.5)	DZQH	3050 (40)	0.69 (0.02)	(4)	Elms et al. (2022)
215406.45−011709.55	39.2 (0.1)	DA+M	9190 (130)	0.58 (0.03)	(1)	Giammichele et al. (2012)
230550.09+392232.88	27.9 (0.1)	DC	4550 (30)	0.698 (0.004)	(2)	Bergeron et al. (2022)
231732.63−460816.77	26.0 (0.3)	DQpec	4080 (100)	0.70 (0.01)	(1)	This work

Notes: (1) *Gaia* photometry contaminated by nearby main-sequence star or unresolved main-sequence companion, (2) IR-faint white dwarf with no unique *Gaia* fit solution, (3) Strong C_2 molecular features affect *Gaia* photometry, (4) Ultra-cool white dwarf.

Table A6. List of wide binaries and higher-order systems, where at least one companion is a white dwarf, within 40 pc. The table is accessible online at this link. The projected separation between sources is given in pc and au, and the tangential velocity difference $delta\_vtan$ is in km/s.

Table A7. Abundances and upper limits of elements determined from combined fitting of spectra and photometry with Koester (2010) models.

Parameter	WD J0213−3345	WD J1154−6239	WD J1927−0355	WD J2141−3300	WD J2317−4608
$T_{\rm eff}$ [K]	5150 (150)	5100 (100)	6540 (150)	6870 (150)	4075 (100)
$\log(g)$ [cm s^{-2}]	7.6 (0.2)	7.97 (0.05)	7.99 (0.04)	7.96 (0.04)	8.2 (0.2)
Composition, X	H	H	He	He	He
log(H/X)	–	–	−3.5	−3.5	–
log(C/X)	–	–	–	–	−8.3 (1.0)
log(Na/X)	–	–	< −9.4	−9.2 (0.2)	–
log(Mg/X)	–	–	−7.00 (0.15)	−7.50 (0.15)	–
log(Al/X)	–	–	< −8.6	−8.5 (0.3)	–
log(Si/X)	–	–	< −7.6	−7.2 (0.2)	–
log(Ca/X)	−10.9 (0.1)	−11.1 (0.2)	−9.1 (0.11)	−8.9 (0.1)	–
log(Sc/X)	–	–	< −11.7	< −11.7	–
log(Ti/X)	–	–	−10.7 (0.1)	−10.0 (0.1)	–
log(V/X)	–	–	< −10.5	< −10.4	–
log(Cr/X)	–	–	−10.2 (0.2)	−10.0 (0.2)	–
log(Mn/X)	–	–	< −9.2	< −9.3	–
log(Fe/X)	–	–	−8.0 (0.1)	−8.2 (0.1)	–
log(Co/X)	–	–	< −11.0	< −10.7	–
log(Ni/X)	–	–	−9.3 (0.2)	−9.2 (0.2)	–
log(Cu/X)	–	–	< −11.7	< −11.7	–
log(Sr/X)	–	–	< −12.3	−12.1 (0.3)	–
log(Ba/X)	–	–	< −12.2	< −12.2	–

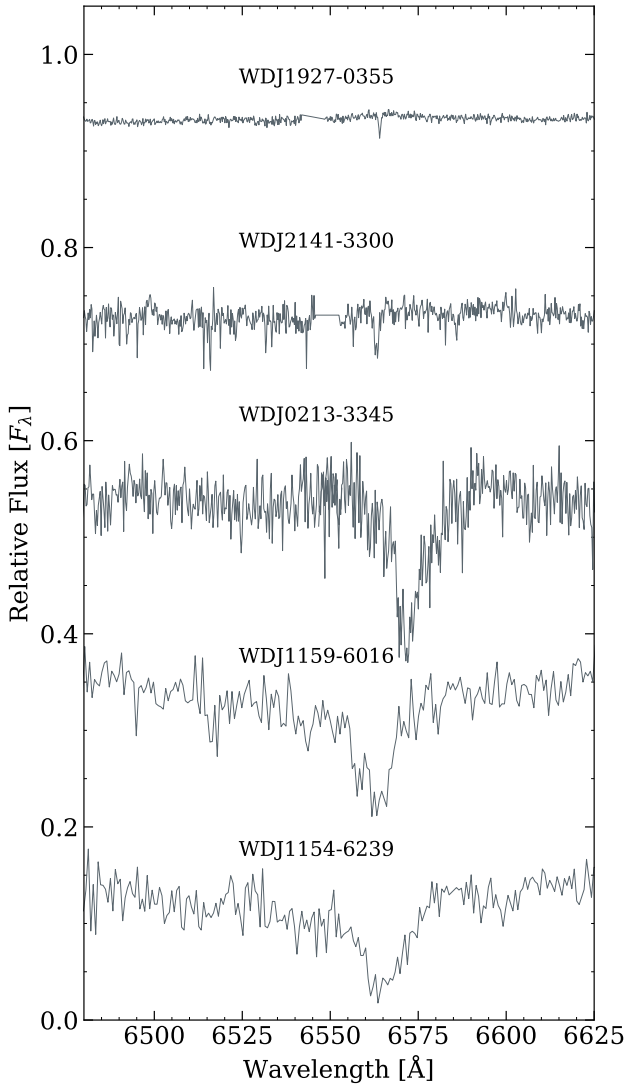

Figure A3. Hα-line spectra from HIRES (first and second), MIKE (third) and MagE (fourth and fifth) observations of **WD J1927−0355**, **WD J2141−3300**, **WD J0213−3345**, **WD J1159−6016** and **WD J1154−6239**.

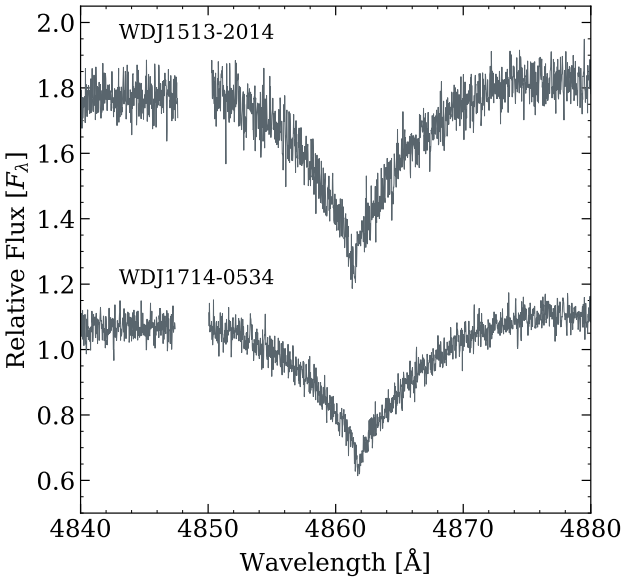

Figure A4. Hβ-line spectra from HIRES observations of **WD J1513−2014** and **WD 1714−0534**.

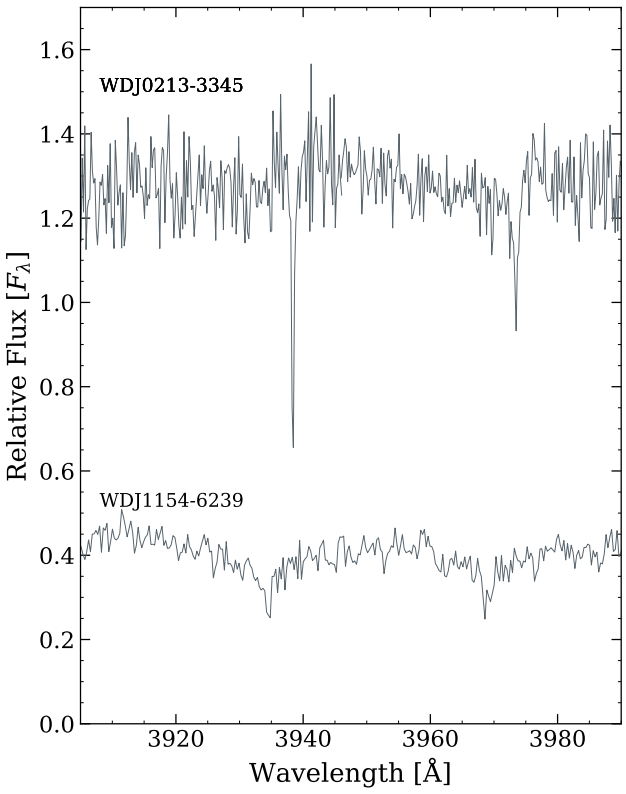

Figure A5. Ca II H+K-line spectra from MIKE (top) and MagE (bottom) observations of **WD J0213−3345** and **WD J1154−6239**. Both spectra are of DAZ white dwarfs with intrinsic calcium absorption.

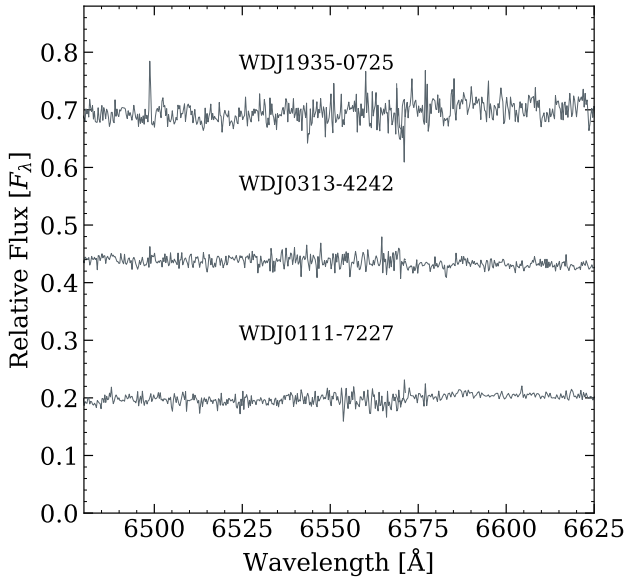

Figure A6. Spectra from MIKE of **WD J1935−0725**, **WD 0313−4242**, and **WD 0111−7227**, which are all DC white dwarfs showing no hydrogen features around the Hα region.

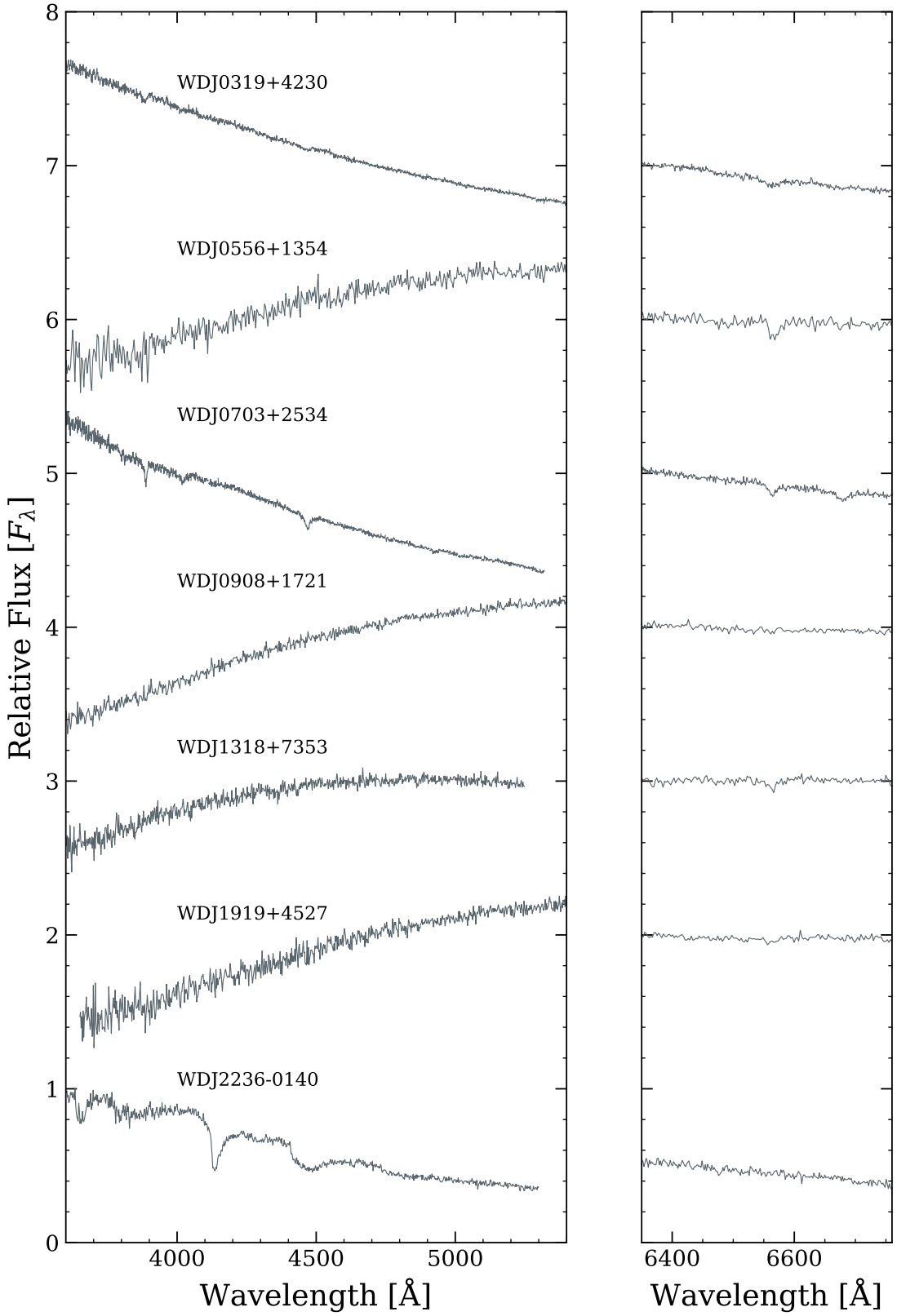

Figure A7. Spectra of white dwarfs observed with Kast.

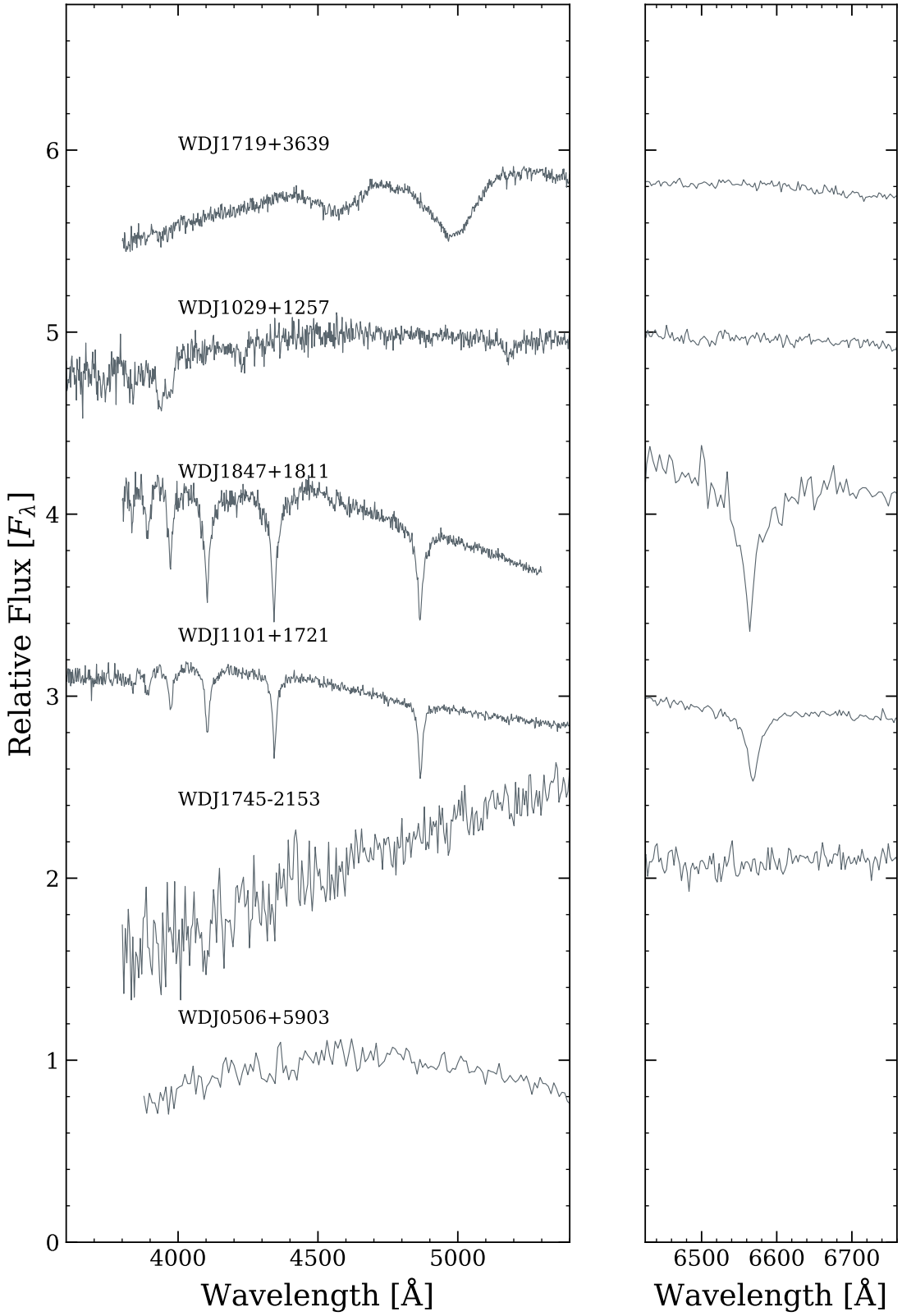

Figure A8. Spectra of white dwarfs observed with Kast.